Atmos. Chem. Phys. Discuss., 12, 6485–6517, 2012
www.atmos-chem-phys-discuss.net/12/6485/2012/
doi:10.5194/acpd-12-6485-2012

Atmospheric Chemistry and Physics Discussions

Implications of the O + OH reaction in hydroxyl nightglow modeling

P. J. S. B. Caridade[1], **J.-Z. J. Horta**[1,2], **and A. J. C. Varandas**[1]

[1]Departamento de Química, Universidade de Coimbra, 3004-535 Coimbra, Portugal
[2]permanent address: Universidad Camilo Cienfuegos, Matanzas, Cuba

Received: 1 February 2012 – Accepted: 16 February 2012 – Published: 1 March 2012

Correspondence to: A. J. C. Varandas (varandas@qtvs1.qui.uc.pt)

Published by Copernicus Publications on behalf of the European Geosciences Union.

Abstract

The hydroxyl nightglow has been examined anew using more realistic estimates of the rate constants for the key reactive and inelastic OH(v') + O quenching processes, which have been obtained from quasiclassical trajectories run on the adiabatic ab initio-based realistic DMBE-IV potential energy surface for the ground state of the hydroperoxil radical. Significant differences in the vertical profiles of vibrationally excited hydroxyl radicals are obtained relative to the ones predicted by Adler-Golden (1997) when employing an OH(v') + O effective rate constant fixed at twice the experimental value for $v' = 1$. Other limiting cases reported in the literature are also discussed. Additionally, the validity of the steady-state hypothesis is analysed by comparing with the results obtained via numerical integration of the master equations.

1 Introduction

Numerous mysteries in terrestrial atmosphere (Crutzen, 1997), most still unsolved, stimulated the study of reactions and chemical cycles (Slanger et al., 1988; Toumi et al., 1996; Varandas, 2002, 2005b) focusing regions (such as stratosphere and mesosphere) that are critical for the sustainability of life on Earth. One important contribution arises from the non-local thermodynamic equilibrium or non-LTE hypothesis (also referred to in previous work and hereinafter by local thermodynamic disequilibrium or LTD (Varandas, 2003)) for the molecular internal degrees of freedom (López-Puertas and Taylor, 2001). The concept of non-LTE was introduced in the context of stellar atmospheres by Milne (1930), while Spitzer Jr. (1949) first pointed out the possibility that at the low pressures found in the upper atmosphere, the radiative field could upset the state of LTE. The first application of a non-LTE formulation in the terrestrial atmosphere was by Curtis and Goody (1956) in their study of the CO_2 15 µm cooling rate in the mesosphere.

ACPD

12, 6485–6517, 2012

Due to the physical chemistry properties at high atmospheric altitudes, namely low pressures and temperatures, the lifetime of vibrationally excited molecules may be substantial. Assuming non-LTE, the chemistry changes dramatically due to the internal energy contents of the species involved: endothermic reactions become exothermic with rate constants substantially larger, reaching orders of magnitude (Silveira et al., 2004; Varandas, 2005b). Although several studies have been devoted to the role of vibrationally excited species in reactions, particularly for the HO_x cycle, atmospheric models of the stratosphere and upper layers neglect non-LTE (see, e.g. von Clarmann et al., 2010, and references therein). One of the reasons pointed out (McDade et al., 1987; Adler-Golden, 1997) is the lack of accurate state-to-state deactivation and state-dependent chemical reactivity for key reactions involved in the atmospheric cycles. Another reason is associated to the non-existence of accurate vertical profiles of vibrational excited species.

An important manifestation of excited molecules and non-LTE in the atmosphere is the cooling down from radiative vibrational-rotational transitions within the $^2\Pi$ electronic state of the hydroxyl radical. The intense emission dominates the nightglow visible spectrum and has been first reported by Meinel (1950) becoming known as Meinel bands. Although more than 60 yr have elapsed, a full understanding of the hydroxyl nightglow has not been achieved.

It is common wisdom that the production of vibrationally excited hydroxyl radical is the outcome of the Bates and Nicolet (1950) mechanism

$$H + O_3 \rightarrow OH(v) + O_2 \qquad \text{(R1)}$$

The nascent OH is produced mostly in high vibrational states (Charters et al., 1971; Murphy, 1971; Ohoyama et al., 1985), $v = 7$, 8, peaking at 9. The mechanism leading to the population of lower states, which are responsible for the intense Meinel bands emission, is still a subject of controversy (McDade et al., 1987). The lower vibrational states can be produced through radiative emission

$$OH(v') \rightarrow OH(v'') + h\nu \qquad \text{(R2)}$$

ACPD
12, 6485–6517, 2012

and/or by collisional deactivation

$$OH(v') + Q \rightarrow OH(v'') + Q \quad \text{(R3)}$$

where Q is the quencher. McDade and LLewellyn (1987) suggested two limiting cases for the relaxation of the hydroxyl radical via Reaction (R3). The first model, denoted by "sudden-death", assumes that any relaxation process does not contribute to the population of lower states, i.e. a chemical quenching process. The second, "collisional cascade", assumes that the lower states are obtained via one-quantum vibrational transitions. Using these two limiting cases, several groups (McDade and LLewellyn, 1988; Melo et al., 1997) obtained effective reaction and vibrational relaxation rate constants by analysing the emission volume of the 8-3 Meinel band. The data inversion of McDade and LLewellyn (1987) based on ground-based observations led to the description the altitude-integrated OH vibrational distribution, but may not necessarily be consistent with altitude profiles of the individual levels (McDade et al., 1987).

The rationalization of the nightglow spectrum is strongly dependent on the kinetics data and vertical profiles of OH(v), being particularly relevant in the case of atmospheric remote sensing (Pickett and Peterson, 1996). Major difficulties arise from the inaccuracies in the absolute Einstein coefficients for the hydroxyl spontaneous emission and the use of different vibrational and reactive rate constants. For example, early work (Finlayson-Pitts and Kleindienst, 1981; Greenblatt and Wiesenfeld, 1982) suggests that many of the used vibrational deactivation rate coefficients may have serious errors, and the conclusions regarding the Meinel bands could be erroneous (McDade, 1991).

One of the references for atmospheric modelling is the work by Adler-Golden (1997), hereinafter also abbreviated as AG. Using experimental observations, a new set of state-to-state vibrational relaxation rate constants and Einstein coefficients has been proposed to be consistent with the laboratory measurements. Although reproducing the satellite observations of the nightglow (McDade et al., 1987), a limitation of this work (Adler-Golden, 1997) refers to the O + OH(v) reaction. Since the relaxation rate

ACPD
12, 6485–6517, 2012

constant for $v > 1$ was unknown, a vibrationally independent effective quenching has been fixed at twice the value of the experimental total removal rate (Spencer and Glass, 1977). Such a value has been confirmed (Pickett et al., 2006) by means of upper atmospheric measurements, but its use has been criticized (von Clarmann et al., 2010) since it leads to a smaller population of hydroxyl radical than the observed one. For this, it has been stated (von Clarmann et al., 2010) that it may provide an upper limit for the reaction.

To assess the role of the $O + OH(v)$ reaction in the OH nightglow modelling, accurate and reliable state-to-state vibrational relaxation and state-specific O_2 formation rate constants are required. Using quasi-classical trajectories, a detailed dynamical study under non-LTE conditions has been reported by Varandas (2004a, 2007). This work will be revisited and implications of the $O + OH(v)$ reaction in atmospheric modelling analysed. For this, the reported (Varandas, 2004a, 2007) state-specific rate constant for the O_2 formation will be employed. Using the results obtained from the batches of trajectories that have been run (Varandas, 2004a, 2007), state-to-state vibrational relaxation rate constants for the $O + OH(v)$ reaction have been extracted for temperatures ranging from 160K to 300K, which will be presented in Sect. 2. Analysis of the vibrationally excited hydroxyl radical vertical profiles is then carried out using the steady-state hypothesis for the kinetics mechanism reported in Sect. 3. To assess the validity of the steady-state condition, the numerical integration of the differential equations has also been performed. Section 4 gathers the major results and discussion.

2 The O+OH(v) reaction

The $O + OH$ reaction has been widely studied experimentally as it is the masterpiece in many interdisciplinary areas (Miller et al., 1990; Smith et al., 2004; Varandas, 2007). Despite its relevance, most theoretical studies have focused on the reactive component by assuming a Boltzmann distribution for the internal degrees of freedom. To

ACPD
12, 6485–6517, 2012

overcome this gap, a detailed study has been performed (Varandas, 2004a, 2007) for both reactive

$$O + OH(v') \rightarrow O_2 + H \quad \text{(R4)}$$

and vibrational quenching

$$O + OH(v') \rightarrow O + OH(v'') \quad \text{(R5)}$$

by using quasiclassical trajectory (QCT) methods (Hase et al., 1996) at temperatures between 110 and 450K. The details of such state-specific O + OH vibrational calculations, which have been here re-analyzed, can be found in Varandas (2004a). Thus, we will only focus the relevant aspects concerning the present work.

The calculations employed the QCT method and the widely used double many-body potential energy surface (Pastrana et al., 1990) (DMBE IV) for $HO_2(^2A'')$. The DMBE IV form is an ab-initio based potential function that has been extensively employed in studies of the O + OH reaction and its reverse, using both quantum (Lin et al., 2006) and classical (Varandas, 2005b) methods. Indeed, special care has been taken to achieve a realistic description of the atom-diatom long-range forces, with the inclusion of dispersion and electrostatic energy components. Although new surfaces have been reported (Xie et al., 2007) from high-level ab initio methods, they may not describe so well the long-ranges forces since they are based on interpolation schemes and rely on the accuracy of the raw data. In fact, despite having been published in 1990, DMBE IV remains amongst the reference PESs in the literature (Lin et al., 2006) for $HO_2(^2A'')$.

The calculations by method I reported elsewhere (Varandas, 2004a) use for each temperature a steady-state distribution that mimics the vibrational states of OH in the upper atmosphere (Varandas, 2003), while, for rotation, effective nascent rotational micro-populations for the six OH Meinel bands (4-0, 5-1, 6-1, 7-2, 8-3, 9-4) have been utilized (private communication by P. C. Cosby in Varandas, 2004a). The final vibrational state analysis of the OH and O_2 has then been carried out semi-classically (Hase et al., 1996). To check for fluctuations in the rate constant due to statistical errors

ACPD
12, 6485–6517, 2012

reported in the original work (Varandas, 2004a), additional trajectories have been integrated but the numerical values remain within the significant figures of the reported rate constants.

The rate constant for vibrational quenching is calculated using the expression

$$k_{(R5)}^{v'\to v''} = g_e(T)\left(\frac{8k_B T}{\pi\mu}\right)^{1/2} \pi b_{max}^2 N^{v'\to v''}/N^{v'} \quad (1)$$

where k_B is the Boltzmann constant, μ the reduced mass of the reactants, b_{max} the maximum impact parameter, $N^{v'\to v''}$ the number of trajectories in a total of $N^{v'}$ trajectories, and $g_e(T) = 2\{[5+3\exp(-228/T)+\exp(-326/T)][2+2\exp(-205/T)]\}^{-1}$ the electronic degeneracy factor taking into account the fine structure of $O(^3P)$ and $OH(^2\Pi)$. A similar expression can be derived for the reactive part, Reaction (R4), substituting $N^{v'\to v''}/N^{v'}$ by the reactive probability. Table 1 gathers the state-to-state vibrational-relaxation and state-specific rate constants for $H+O_2$ formation. Note that both the inelastic

$$O_a + O_bH(v') \to O_a + O_bH(v'') \quad (R6)$$

and atom-exchange reactive channels

$$O_a + O_bH(v') \to O_b + O_aH(v'') \quad (R7)$$

count as vibrational relaxation processes when $v' \neq v''$. For comparison, total removal rate constants reported in Varandas (2004a, 2007) are also shown in Table 1.

A well known problem in QCT, is that the method cannot account for quantum mechanical effects. For example, since we are dealing with a light atom, tunnelling can be an important issue. However, the calculated rate constants are mostly found in good agreement with the best reported data, and such evidence is even valid for systems as light as $H+H_2$ (Zhao et al., 1990). Another issue that cannot be overlooked in QCT methods is the problem of zero-point energy leakage, with the reader being referred

ACPD
12, 6485–6517, 2012

to Varandas (2007) for earlier work on this topic. Due to the high exoergicity, ZPE leakage should be negligible for the title reaction.

A salient feature of the data reported in Table 1 is the importance of multi-quanta transitions for the vibrational relaxation over the whole range of temperatures. In particular, for high vibrational quantum numbers the rate constant is, within the statistical error, almost constant irrespectively of the vibrational state. For low vibrational quantum states, $v' = 1$ for example, the tendency is to diminish with temperature. For a better comparison between the two competing processes, Fig. 1 shows the branching ratios $\eta_{v'}(T) = k^{v'}_{(R4)}(T)/k^{v'\rightarrow all}_{(R5)}(T)$. It can be seen that they display a rough T-independent pattern, with $\eta_{v'}$ increasing sharply with the initial quantum number for $v' \geq 6$.

In all cases, the dominant contribution for large v' is the reactive contribution. This can be rationalized from the highly stretched OH molecule in these cases, which favours bond-breaking. Moreover, the reactive rate constant has been rationalized at low temperatures by a capture model due to the prevailing long-range forces (Clary and Werner, 1984; Varandas, 1987). One then expects the rate constant to decrease with temperature. Also relevant is the enhancement of the rate constant for $H + O_2$ formation with increasing v'.

Khachatrian and Dagdigian (2005) reported a total removal rate constant for OH($v = 1$) at room-temperature of $3.9 \pm 0.6 \times 10^{-11}\,cm^3 s^{-1}$, with the recommended values of IUPAC (Atkinson et al., 2004) and NASA (Sander et al., 2006) being 3.5 ± 0.1 and $3.3 \pm 0.7 \times 10^{-11}\,cm^3 s^{-1}$, respectively. The QCT result (Varandas, 2004a) for $T = 255$K [300K] is $(4.6 \pm 0.2) \times 10^{-11}\,cm^3 s^{-1}$ [$(4.0 \pm 0.3) \times 10^{-11}\,cm^3 s^{-1}$], in very good agreement with the experimental and recommended values. The value utilized by Adler-Golden (1997) comes from the experimental work of Spencer and Glass (1977) [$(4.5 \pm 1.3) \times 10^{-11}\,cm^3 s^{-1}$ for vibrational relaxation, and $(10.5 \pm 5.3) \times 10^{-11}\,cm^3 s^{-1}$ for reaction], having employed for the total relaxation constant a value of $20 \times 10^{-11}\,cm^3 s^{-1}$. Clearly, his value overestimates by far both the experimental/recommended and this work theoretical data. Marshall et al. (2002) studied the relaxation of OH(v') by laser-induced fluorescence, having reported a preliminary value of $k = 4.6 \times 10^{-11}\,cm^3 s^{-1}$ for $v' = 2$ at

ACPD
12, 6485–6517, 2012

room-temperature. The QCT result is $k(T = 255\,\mathrm{K}) = (5.1 \pm 0.1) \times 10^{-11}\,\mathrm{cm^3 s^{-1}}$ (Varandas, 2004a) and $(4.8 \pm 0.1) \times 10^{-11}\,\mathrm{cm^3 s^{-1}}$ for $T = 300\,\mathrm{K}$, again in good agreement with experiment.

3 Kinetics mechanism and input data

For altitudes between 80 and 100 km, it is commonly accepted that vibrationally excited OH radicals are produced essentially via the Bates and Nicolet (1950) mechanism:

$$H + O_3 \rightarrow OH(v') + O_2 \quad \text{(R8)}$$

with the product OH showing an inverted vibrational distribution that peaks at $v' = 9$. In turn, the standard ozone source is the fast three-body recombination process

$$O + O_2 + M \rightarrow O_3 + M \quad \text{(R9)}$$

where $M = N_2$, O_2, and O, are all in the ground electronic state. While the rate of $OH(v')$ formation can be equated to the one of ozone formation, Reaction (R9), the most important depletion processes of $OH(v')$ are

$$OH(v') + O_2 \rightarrow OH(v'') + O_2 \quad \text{(R10)}$$
$$OH(v') + N_2 \rightarrow OH(v'') + N_2 \quad \text{(R11)}$$
$$OH(v') + O \rightarrow OH(v'') + O \quad \text{(R12)}$$
$$OH(v') + O \rightarrow O_2 + H \quad \text{(R13)}$$
$$OH(v') \rightarrow OH(v'') + h\nu \quad \text{(R14)}$$

The mechanism defined by Reaction (R8) to (R14) can be generalized to account for other sources and sinks of O_3 and $OH(v)$. For example, although it has been noted (Adler-Golden, 1997) that the reaction $O + HO_2$ could be a potential candidate, previous work (Kaye, 1988) has shown that it may not play a crucial role in studies of the high atmosphere. Although this assumption is possibly valid for HO_2 in the ground

ACPD
12, 6485–6517, 2012

vibrational state as the dynamics only yields OH($v' \leq 6$), the argument no longer holds if non-LTE is considered, since up to OH($v = 15$) products can then be formed (Silveira et al., 2004; Varandas, 2005b). In addition, the reaction of $OH + O_3$ has been shown to yield HO_2 vibrationally excited above the classical asymptote for dissociation, thus being another potential source of OH(v') (Varandas and Zhang, 2001; Zhang and Varandas, 2001). Furthermore, from the so-called HO_{y+3} mechanisms (Varandas, 2002), one may have to pay attention to the reaction $OH(v') + O_2(v'')$ as a potential sink of vibrationally excited OH. For the sake of discussion and comparison (Adler-Golden, 1997), such extra complications will be here left aside.

From Reaction (R8) to (R9) and using the steady-state assumption for O_3, one gets:

$$k_{(R8)}[H][O_3] = \sum_M k^M_{(R9)}[O][O_2][M] \tag{2}$$

while for the [OH(v')] the result is:

$$\begin{aligned}[OH(v')]_{CHV} = \Big\{ & \omega_{OH(v')} \sum_M k^M_{(R9)}[O][O_2][M] + \\ & k^{v'+1\leq 9 \rightarrow v'}_{(R11)}[N_2][OH(v'+1 \leq 9)] + \\ & \sum_{v^*=v'+1}^{9} \left[k^{v^* \rightarrow v'}_{(R10)}[O_2] + k^{v^* \rightarrow v'}_{(R12)}[O] + A_{v' \leftarrow v^*}\right] \times \\ & [OH(v^*)]\Big\} \Big\{ k^{v' \rightarrow v'-1}_{(R11)}[N_2] + k_{(R13)}[O] + \\ & \sum_{v^*=0}^{v'-1} \left[k^{v' \rightarrow v^*}_{(R10)}[O_2] + k^{v' \rightarrow v^*}_{(R12)}[O] + A_{v' \leftarrow v^*}\right] \Big\}^{-1} \end{aligned} \tag{3}$$

where $A_{v' \leftarrow v''}$ are the Einstein coefficients for spontaneous emission of Reaction (R14), and $\omega_{OH(v')}$ the nascent distribution of OH(v') states. The vertical profiles can be evaluated recursively starting from $v' = 9$. Thus, the contributions that originate from

ACPD
12, 6485–6517, 2012

relaxation of higher v' states have been considered as a source of OH($v' \leq 8$) but discarding any excitation from lower v' states. This can be justified by lacking, to the best of our knowledge, of reliable estimates for such state-to-state vibrational-excitation rate constants, which are anyway expected to be very small at the temperatures of interest (Varandas, 2004a). Of course, collisional processes involving vibrationally excited O_2 and other species (Caridade et al., 2002; Varandas, 2005b) are left aside in this judgement.

Using the steady-state hypothesis for the same set of reactions, but the Adler-Golden assumption for Reactions (R12) and (R13) (i.e. cascading via Reaction (R12) is absent), the result is:

$$
\begin{aligned}
[\mathrm{OH}(v')]_{\mathrm{AG}} = & \left\{ \omega_{\mathrm{OH}(v')} \sum_{M} k^{M}_{(\mathrm{R9})} [\mathrm{O}][\mathrm{O_2}][M] + \right. \\
& k^{v'+1 \leq 9 \rightarrow v'}_{(\mathrm{R11})} [\mathrm{N_2}][\mathrm{OH}(v'+1 \leq 9)] + \\
& \left. \sum_{v^*=v'+1}^{9} (k^{v^* \rightarrow v'}_{(\mathrm{R10})} [\mathrm{O_2}] + A_{v' \leftarrow v^*}) [\mathrm{OH}(v^*)] \right\} \times \\
& \left\{ k^{v' \rightarrow v'-1}_{(\mathrm{R11})} [\mathrm{N_2}] + \sum_{v^*=0}^{v'-1} \left[k^{v' \rightarrow v^*}_{(\mathrm{R10})} [\mathrm{O_2}] + \right. \right. \\
& \left. \left. k^{v'}_{(\mathrm{R12})+(\mathrm{R13})} [\mathrm{O}] + A_{v' \leftarrow v^*} \right] \right\}^{-1} \qquad (4)
\end{aligned}
$$

with $k^{v'}_{(\mathrm{R12})+(\mathrm{R13})} = 2 \times 10^{-10}\,\mathrm{cm^{-3}\,s^{-1}}$ as a v'-independent effective quenching rate constant.

In turn, the "sudden-death" vertical profiles of McDade and LLewellyn (1987) assume the form

$$
[\mathrm{OH}(v')]_{\mathrm{sd}} = \left\{ \omega_{\mathrm{OH}(v')} \sum_{M} k^{M}_{(\mathrm{R9})} [\mathrm{O}][\mathrm{O_2}][M] + \right.
$$

ACPD
12, 6485–6517, 2012

$$\sum_{v^*=v'+1}^{9} A_{v'\leftarrow v^*}[\mathrm{OH}(v^*)]\Big\}\Big\{(k_{(\mathrm{R12})}^{v'\rightarrow 0}+k_{(\mathrm{R13})})[\mathrm{O}]+$$

$$k_{(\mathrm{R10})}^{v'\rightarrow 0}[\mathrm{O_2}]+\sum_{v^*=0}^{v'-1} A_{v'\leftarrow v^*}\Big\}^{-1} \quad (5)$$

having the emission process Reaction (R14) as the only source of low OH vibrational states, while their "collisional cascade" mechanism leads to:

$$[\mathrm{OH}(v')]_{\mathrm{cc}} = \Big\{\omega_{\mathrm{OH}(v')}\sum_{M} k_{(\mathrm{R9})}^{M}[\mathrm{O}][\mathrm{O_2}][M]+(k_{(\mathrm{R11})}^{v'+1\rightarrow v'}[\mathrm{N_2}]+$$

$$k_{(\mathrm{R10})}^{v'+1\rightarrow v'}[\mathrm{O_2}]+k_{(\mathrm{R12})}^{v'+1\rightarrow v'}[\mathrm{O}])[\mathrm{OH}(v'+1)]+$$

$$\sum_{v^*=v'+1}^{9} A_{v'\leftarrow v^*}[\mathrm{OH}(v^*)]\Big\}\Big\{k_{(\mathrm{R11})}^{v'\rightarrow v'-1}[\mathrm{N_2}]+$$

$$k_{(\mathrm{R13})}[\mathrm{O}]+k_{(\mathrm{R10})}^{v'\rightarrow v-1}[\mathrm{O_2}]+k_{(\mathrm{R12})}^{v'\rightarrow v-1}[\mathrm{O}]+$$

$$\sum_{v^*=0}^{v'-1} A_{v'\leftarrow v^*}\Big\}^{-1} \quad (6)$$

In this case, besides the population arising from Reaction (R14), other sources of $\mathrm{OH}(v')$ are the one-quantum relaxation Reactions (R10), (R11) and (R12).

The temperature and concentration profiles here employed have been taken from NRLMSISE 2000 which gathers revised $\mathrm{O_2}$ and O densities in the lower thermosphere (Hedin, 1987). To compare with experimental measurements we have used the conditions present in the multiple rocket investigation of the nightglow, also know as ETON, version 5 (McDade et al., 1987). The parameters considered in the profile database were: 23 March 1982, 57.36° N, 352.62° E and 23:28:23 UTC, the conditions of ETON5. The uncertainties in temperature and molecular concentrations are of about 10 K and

ACPD
12, 6485–6517, 2012

10 %, respectively. In turn, the nascent distribution of OH(v') states for Reaction (R8) are taken from a renormalization (Adler-Golden, 1997) of the data of Charters et al. (1971); see Fig. 2. Such values have been extrapolated to lower v' states using information theory (Steinfeld et al., 1987), and renormalized to the Einstein coefficients of Nelson et al. (1990). Additionally, the three-body recombination rate constants have been taken from Atkinson et al. (2004) which are valid for the temperature range 100–300 K, thus embracing the limits investigated in this work of 169 K and 206 K for altitudes between 80 and 100 km, respectively. As for the OH(v') + O_2 and OH(v') + N_2 reactions, we have used unaltered the semi-empirical data (Adler-Golden, 1997). Although classical trajectories have been run in our group (Garrido et al., 2002; Caridade et al., 2002) for the OH(v') + O_2(v'') reactive and non-reactive processes, no accurate data has yet been reported for the state-to-state vibrational relaxation of OH(v') in collisions with O_2($v = 0$). To account for the influence of variation in temperature on the O + OH(v') rate constants along the vertical profile, a simple interpolation scheme has been utilized.

Key elements for the description of the OH profiles are the Einstein transition probabilities for radiative transitions. The most used in atmospheric modelling come from the work of Nelson et al. (1990), from laboratory measurements of $\Delta v = 1$ and $\Delta v = 2$. They have been reported (Adler-Golden, 1997) as the most accurate at the time, although for higher overtones the data show strong deviations. Other data sets have been reported in the literature (Turnbull and Lowe, 1989; Langhoff et al., 1986; Murphy, 1971), but all with limitations. Based on the fact that the method used by Turnbull and Lowe (1989) should in principle give accurate results, a correction curve has been reported to scale the rotational average data (Adler-Golden, 1997). Such a correction was based on an inaccurate intensity calibration which leads to a systematic error in function of the band-center frequency.

Rather than using the above data sets, we have adopted the newly calculated Einstein transition probabilities of van der Loo and Groenenboom (2007, 2008) based on accurate ab initio data. Using Hund's case (a) for the OH radical (Huber and Herzberg,

ACPD
12, 6485–6517, 2012

1979), each vibrational state wave function $|JM_J{}^2\Pi_{|\Omega|}p\rangle$, is characterized by $\boldsymbol{J}$, the total angular momentum, M_J, the projection of the vector $\boldsymbol{J}$ on the laboratory-frame Z-axis, $|\Omega| = 1/2, 3/2$, the total electronic angular momentum projection on the molecular axis and $p = \pm 1$ the spectroscopic parity operator. Since for low rotational states, Ω is a good quantum number, the wave function is usually labeled by F_1 when $\Omega = 3/2$ and F_2 for $\Omega = 1/2$. In their work (van der Loo and Groenenboom, 2007, 2008) they reported 24 660 Einstein coefficients and photoabsorption cross sections for the full set of quantum numbers $\{v, J, F_n, p\}$ for upper and lower states up to $v = 10$. The specific rotational band intensities for the $P(J')$, $Q(J')$ and $R(J')$ bands, $J'' = J' + 1$, $J'' = J'$, and $J'' = J' - 1$, respectively, have been calculated up to $J = 121/2$. The computed lifetimes reported using such data lie between the best known experimental values, with the error in the calculated frequencies being of $\sim 0.05\%$.

If we assume a Boltzmann distribution of the rotational states at T_{rot}, the thermally average radiative transition probability for the vibrational band $v'' \leftarrow v'$ is defined as (Mies, 1974)

$$A_{v''\leftarrow v'}(T_{\mathrm{rot}}) = Q_{v'}^{-1}(T_{\mathrm{rot}}) \sum_{J',F_n',p',J'',F_n'',p''}^{\mathrm{all}} (2J'+1) \times A(p'', F_n'', J'', v'' \leftarrow p'', J', F_n', v') \times \exp(-E_{v';J',F_n',p'}/k_{\mathrm{B}}T_{\mathrm{rot}}) \quad (7)$$

with $Q_{v'}(T_{\mathrm{rot}})$ the electronic-rotational partition function assuming the form:

$$Q_{v'}(T_{\mathrm{rot}}) = \sum_{J',F_n',p'}^{\mathrm{all}} (2J'+1)\exp(-E_{v';J',F_n',p'}/k_{\mathrm{B}}T_{\mathrm{rot}}) \quad (8)$$

and "all" implying a summation over all available states. Following Wallace (1962), the equivalence of the gas temperature and rotational temperature has been assumed. Although being in general much weaker than the intramultiplets ($p'' = p'$) bands, the satellite bands, intermultiplet transitions with $p'' \neq p'$ have also been included.

ACPD
12, 6485–6517, 2012

4 Implications of the O+OH reaction on the OH(v) profiles

Using the steady-state hypotheses and the data reported in the previous sections, Fig. 2 shows the distribution of the vibrational excited hydroxyl radical for two altitudes, $h = 90$ and 100 km. For 90 km the vibrational distribution shows an exponential decay with 40 % of the population at the $v = 1$ state, being this trend consistent with all models considered in this work. However, the use of the AG effective rate constant for Reactions (R12) and (R13) predicts nearly 50 % less for $v = 1$, becoming the major contribution after $v = 3$. This clearly shows that the O + OH(v) reaction plays an important role for the description of the vertical vibrational excited hydroxyl radical, specially for lower v states. To reinforce such a statement, the AG assumption has also been revisited, hereafter denoted as AGr, using an effective rate constant with the data here reported, i.e.

$$k^{v}_{(R12)+(R13)}(T) = k^{v}_{(R13)}(T) + k^{v\to 0}_{(R12)}(T) \quad (9)$$

The results nearly coincide with those of multi-quantum cascade, since the reactive rate constant Reaction (R13) is dominant (see Fig. 1). Another salient feature is the larger value of the $v = 1$ population when considering the collisional-cascade mechanism, a fact arising from the larger one-quantum rate constants for lower states (see Table 1).

For 100 km the distribution is more flat, with the population of lower vibrational states reduced to nearly 25% for $v = 1$. In this case, the AG predictions show an almost negligible population of $v = 1$, while for $v = 9$ it is almost of the same order of magnitude of the single-collision results. For comparison, the nascent (Ohoyama et al., 1985) and steady-state distributions reported from single collision trajectory dynamics (Varandas, 2003) are also shown in Fig. 2. Although the vibrational distribution reported in this work is far from a thermalized one (supporting in some extent a previous observation (Varandas, 2003)), it is significantly different from both of them. The differences with respect to the latter are probably due to the fact that this considered only the O + OH(v') reactions as a source of vibrational deactivation, thus providing a kind of limit to the global kinetics model.

ACPD
12, 6485–6517, 2012

The OH(v') vertical profiles for specific vibrational states are shown in Fig. 3 as a function of altitude. The dominant contribution arises from $v = 1$ with the maximum value arising at ∼ 87 km, while for other vibrational states, the maximum is shifted upwards. This can be attributed to the increase of the atomic oxygen concentration and a decrease of the O_2 one, thus reducing the contribution of vibrational relaxation. For a direct comparison with previous results, we have also plotted the total vibrational excited hydroxyl concentration. A fair agreement is observed between the total vertical profile from the current work and the one reported elsewhere (Varandas, 2004b), where stretched oxygen and odd hydrogen species have also been included (Varandas, 2002, 2003, 2004b, 2005a,b) in an attempt to offer a clue for explaining the so-called 'ozone deficit problem' and 'HOx dilemma' in the middle atmosphere under LTD.

Figure 4 gathers the vertical profiles that result from the various models and rate constants reported in the present work. Comparing panel (a) with panel (b), it is clearly visible the role of the O + OH reaction, as already noted. Around 92 km, AG predicts a population inversion, with $v = 1$ being the less populated state, while AGr shows a similar trend with those of Fig. 3. For the "sudden-death" and "collisional-cascade" models, the relative positioning of the vertical profiles is according to the vibrational levels of the hydroxyl radical, although in the "sd" the vibrationally excited populations are substantially smaller for altitudes higher than 90 km, which is due to the chemical quenching nature of the model. Although not shown (cf. Fig. 3), the behaviour of the total concentration in the "cc" model lies close to the results from a previous model (Varandas, 2002, 2003, 2004b, 2005a,b), suggesting that such data may be viewed as providing an upper limit to the real case. Note, however, that the physical-chemical contents of the model just referred differ somewhat from the ones here utilized since it has been based on satellite data at the equatorial region where strong semiannual variations may occur.

For a quantitative analysis, we report in Fig. 5 the relative deviation of the AG (Adler-Golden, 1997) results relative to ours, i.e. $\{[\mathrm{OH}(v)]_{\mathrm{AG}} - [\mathrm{OH}(v)]_{\mathrm{CHV}}\}/[\mathrm{OH}(v)]_{\mathrm{CHV}}$. Although our results essentially agree with AG for $v' = 9$, there are significant deviations

ACPD
12, 6485–6517, 2012

for other v values. For high vibrational states and altitudes, the AG results are nearly 10 to 20 % for $v = 9$ and 7, respectively, while for low vibrational states it may reach up to nearly 90 % for $v = 1$. This is due to the fact that we allow for cascading of the total OH(v) at each step, including the significant part that is formed during the cascading process. Thus, the AG predictions underestimate our results. However, our predicted total concentrations of OH(v) show good agreement (within a factor of two or so) with his results. As noted above, a qualitative agreement is also found with the total concentration of OH(v) predicted from the Varandas (2004b, 2005a) LTD model. In summary, significant differences are observed between the OH(v') profiles for specific vibrational states from this work and the AG results, although the differences are meager for the total [OH(v')]. Of course, an improved model employing accurate estimates of the rate constants of all involved vibrational relaxation and reactive channels [in particular those involving collisions of OH(v') with N_2 and O_2] will be required to assess which prediction is most realistic. This calls for further theoretical and experimental work, as the discrepancies between theory and experiment are particularly large in the vibrational relaxation case (Caridade et al., 2002).

Using the vertical profile for $v = 8$ concentration the volume emission for the 8-3 band has been calculated, with the results being reported in Fig. 6. The rotational average Einstein coefficient for the 8-3 transition is obtained from Eq. (7) as a function of altitude via the temperature variation. Also shown in Fig. 6 is the reported data of (Adler-Golden, 1997) and the data calculated in this work using the AG proposed rate constant, together with the eye-extracted data of ETON5 (McDade et al., 1987). The maximum value is achieved at nearly 90 km, a similar trend from the ETON5 although being more intense (270 vs. ∼150 photons cm^{-3} s^{-1}). With increasing altitude all data sets become nearly identical, with the results here reported lying within the experimental error bars.

A critical assumption in this work is the steady-state hypothesis, a condition frequently employed and quite often taken as granted since its proposition in the seminal work of Bodenstein (1913), Chapman and Hunderhill (1913) and Chapman (1930),

ACPD
12, 6485–6517, 2012

with the the latter utlizing it for the rationalization of the ozone layer in the Earth's atmosphere. To check the steady-state condition in the Meinel bands modelling, the set of 9 differential equations corresponding to the vibrational excited hydroxyl concentrations have been simultaneously solved for all altitudes, considering the fast recombination ozone formation Reaction (R9). Several integration methods have been tested, ranging from the simple Euler to the traditional 4th order Runge-Kutta (RK4) and Bulirsch-Stoer ones. No attempt has been made to use (optimize) a variable step method, or utilize specialized methods for stiff equations. Figure 7 shows a typical vibrationally excited concentration variation with time, in this case for $h = 100$ km. The illustrated results have been obtained with the RK4 method, although tests using the simpler Euler method have shown a similar accuracy. In all cases, the steady-state concentrations were taken as the starting point. As expected, the $v = 9$ concentration quickly achieves steady-state by balancing its formation with depletion. Since a cascade model is considered, the last concentration arriving to the steady-state is the one for $v = 1$. Except for $v = 9$, all time variations show a maximum displaced on time with decreasing value of v before reaching the steady-state.

5 Conclusions

Accurate state-to-state vibrational relaxation rate constants for the $O + OH(v')$ have been presented based on early theoretical work (Varandas, 2004a) which employed the quasiclassical trajectory method and the DMBE IV ab initio-based potential energy surface. As in previous work, the values here reported show that the reactive part dominates over the whole range of initial vibrational quantum numbers and temperatures. It is predicted that the total rate constant at room-temperature is significantly smaller than the one used previously for modelling the hydroxyl Meinel bands in the upper stratosphere. Our confidence on the reported results therefore stems from the accuracy of the potential energy surface which warrants high reliability to the predicted state-to-state and state-specific dynamics and kinetics parameters of

ACPD
12, 6485–6517, 2012

the colision processes involving atomic oxygen and hydroxyl radicals in the various vibrational-rotational states.

To assess the role of the title reaction in the hydroxyl Meinel bands, the steady-state hypothesis has been utilized, and a comparison with other rate constants and simplified models presented. The more realistic mechanism is possibly the one that describes the lower vibrational states of OH via assumption of a collisional cascade process. In this regard, the results from the present work differ significantly from the ones obtained by Adler-Golden as confirmed by using a realistic value for the effective total O + OH quenching rate constant. It is also shown that the results from the limiting-case mechanisms suggested by McDade and LLewellin seem to encompass the total [OH(v)] obtained from the model of Varandas (2005a,b). A final remark on the steady-state hypothesis: it has been shown to offer a reliable working ground for the higher stratosphere and mesosphere at least insofar as the title issue is concerned.

Acknowledgements. J. Z. J. H. thanks III (UC) for financial support, and the UMCC, Cuba, for leave of absence. This work has been carried out under the auspices of Fundação para a Ciência e a Tecnologia, Portugal (contracts POCI/QUI/60501/2004 and POCI/AMB/60261/2004).

References

Adler-Golden, S.: Kinetic parameters for OH nightglow modeling consistent with recent laboratory experiments, J. Geophys. Res., 102, 19969–19976, doi:10.1029/97JA01622, 1997. 6487, 6488, 6492, 6493, 6494, 6497, 6500, 6501, 6512, 6514, 6515, 6516

Atkinson, R., Baulch, D. L., Cox, R. A., Crowley, J. N., Hampson, R. F., Hynes, R. G., Jenkins, M. E., Rossi, M. J., and Troe, J.: Summary of Evaluated Kinetic and Photochemical Data for Atmospheric Chemistry, Atmos. Chem. Phys., 4, 1461–1738, doi:10.5194/acp-4-1461-2004, 2004. 6492, 6497

Bates, D. R. and Nicolet, M.: The Photochemistry of Atmospheric Water Vapor, J. Geophys. Res., 55, 301–327, doi:10.1029/JZ055i003p00301, 1950. 6487, 6493

Bodenstein, M.: Eine Theorie der photochemishen reaktionsgeschwindigkeiten, Z. Physik. Chem., 85, 329–397, 1913. 6501

ACPD

12, 6485–6517, 2012

Caridade, P. J. S. B., Sabin, J., Garrido, J. D., and Varandas, A. J. C.: Dynamics of the $OH + O_2$ vibrational relaxation process, Phys. Chem. Chem. Phys, 4, 4959–4969, doi:10.1039/b203101a, 2002. 6495, 6497, 6501

Chapman, D. L. and Hunderhill, L. K.: The interaction of chlorine and hydrogen. The influence of mass, J. Chem. Soc., Trans., 103, 496–508, doi:10.1039/CT9130300496, 1913. 6501

Chapman, S.: A theory of upper-atmospheric ozone, Memoirs Roy. Metereol. Soc., III, 103, 1930. 6501

Charters, P. E., Macdonald, R. G., and Polanyi, J. C.: Formation of vibrationally excited OH by reaction $H + O_3$, Appl. Opt., 10, 1747–1754, doi:10.1364/AO.10.001747, 1971. 6487, 6497, 6512

Clary, D. C. and Werner, H. J.: Quantum calculations on the rate constant for the $O + OH$ reaction, Chem. Phys. Lett., 112, 346–350, doi:10.1016/0009-2614(84)85755-3, 1984. 6492

Crutzen, P.: Mesospheric mysteries, Science, 277, 1951–1952, doi:10.1126/science.277.5334.1951, 1997. 6486

Curtis, A. R. and Goody, R. M.: Thermal variation in the upper atmosphere, Proc. Royal Soc., 193–206, doi:10.1098/rspa.1956.0128, 1956. 6486

Finlayson-Pitts, B. J. and Kleindienst, T. E.: The reaction of hydrogen atoms with ozone as a source of vibrationally excited $OH(X^2\Pi_i)_{v=9}$, J. Chem. Phys., 74, 4533–4543, doi:10.1063/1.441642, 1981. 6488

Garrido, J. D., Caridade, P. J. S. B., and Varandas, A. J. C.: Dynamics study of the $OH + O_2$ branching atmospheric reaction. 4. Influence of vibrational relaxation in collisions involving highly excited species, J. Phys. Chem. A, 106, 5314–5322, doi:10.1021/jp0203245, 2002. 6497

Greenblatt, G. D. and Wiesenfeld, J. R.: Time-resolved emmision studies of vibrationally excited hydroxyl radicals: $OH(X^2\Pi, v = 9)$, J. Geophys. Res., 87, 1145–1152, doi:10.1029/JC087iC13p11145, 1982. 6488

Hase, W. L., Duchovic, R. J., Hu, X., Komornicki, A., Lim, K. F., Lu, D., Peslherbe, G. H., Swamy, K. N., Linde, S. R. V., Varandas, A. J. C., Wang, H., and Wolf, R. J.: VENUS96: A General Chemical Dynamics Computer Program, QCPE Bull., 16, 43, 1996. 6490

Hedin, A. E.: Extension of the MSIS thermophere model into the middle and lower thermophere, J. Geophys. Res., 96, 1159–1172, doi:10.1029/90JA02125, 1987. 6496

Huber, K. P. and Herzberg, G.: Molecular Spectra and Molecular Structure. IV Constants of Diatomic Molecules, Van Nostrand, New York, 1979. 6497

ACPD

12, 6485–6517, 2012

Kaye, J. A.: On the possibility of the reaction $O + HO_2 \rightarrow OH + O_2$ in OH airglow, J. Geophys. Res., 93, 285–288, doi:10.1029/JA093iA01p00285, 1988. 6493

Khachatrian, A. and Dagdigian, P. J.: Vibrational relaxation of OH by oxygen atoms, Chem. Phys. Lett, 415, 1–5, doi:10.1016/j.cplett.2005.08.131, 2005. 6492

Langhoff, S. R., Werner, H., and Rosmus, P.: Theoretical transition probabilities for the OH Meinel system, J. Mol. Spectrosc., 507–529, doi:10.1016/0022-2852(86)90186-4, 1986. 6497

Lin, S. Y., Rackham, E. J., and Guo, H.: Quantum mechanical rate constants for $H + O_2 \rightleftharpoons O + OH$ and $H + O_2 \rightarrow HO_2$ reactions, J. Phys. Chem. A, 110, 1534–1540, doi:10.1021/jp053555v, 2006. 6490

López-Puertas, M. and Taylor, F. W.: Non-local Thermodynamic Equilibrium in the Atmosphere, vol. 3, World Scientific, 2001. 6486

Marshall, J., Kalogerakis, K. S., and Copeland, R. A.: Laboratory measurements of OH(v=2) collisional reactivation by oxygen atoms, American Geophysical Union Spring 2001 meeting, paper SA31A–21, 2002. 6492

McDade, I. C.: The altitude dependence of the OH($X^2\Pi$) vibrational distribution in the nightglow: Some model expectations, Planet. Space Sci., 39, 1049–1057, doi:10.1016/0032-0633(91)90112-N, 1991. 6488

McDade, I. C. and LLewellyn, E. J.: Kinetic parameters related to sources and sinks of vibrationally excited OH in the nightglow, J. Geophys. Res., 92, 7643–7650, doi:10.1029/JA092iA07p07643, 1987. 6488, 6495, 6512, 6514

McDade, I. C. and LLewellyn, E. J.: Mesospheric oxygen atom densities inferred from nighttime OH Meinel band emission rates, Planet. Space Sci., 36, 897–905, doi:10.1016/0032-0633(88)90097-9, 1988. 6488

McDade, I. C., LLewellyn, E. J., Mutagh, D. P., and Greer, R. G. H.: ETON5: simultaneous rocket measurements of the OH Meinel $\Delta v = 3$ sequence and (8,3) band emission profiles in the nightglow, Planet. Space Sci., 35, 1137–1147, doi:10.1016/0032-0633(87)90020-1, 1987. 6487, 6488, 6496, 6501, 6516

Meinel, A. B.: OH emission bands in the spectrum of the night sky. I., Astrophys. J., 111, 555, doi:10.1086/145296, 1950. 6487

Melo, S. M. L., Takahashi, H., Clemesha, B. R., and Simonich, D. M.: An experimental study of the nightglow OH(8-3) band emission process in the equatorial mesosphere, J. Atmos. Sol.-Terr. Phy., 59, 479–486, doi:10.1016/S1364-6826(96)00053-3, 1997. 6488

ACPD

12, 6485–6517, 2012

Mies, F. H.: Calculated vibrational transition probabilities of OH($X^2\Pi$), J. Mol. Spectrosc., 53, 150–188, doi:10.1016/0022-2852(74)90125-8, 1974. 6498
Miller, J. A., Kee, R. J., and Westbrook, C. W.: Chemical kinetics and combustion modelling, Annu. Rev. Phys. Chem., 41, 345–387, doi:10.1146/annurev.pc.41.100190.002021, 1990. 6489
Milne, E. A.: Thermodynamics of stars, Handbuch der Astrophysik, 1930. 6486
Murphy, R. E.: Infrared emission of OH in the fundamental and first overtone bands, J. Chem. Phys., 54, 4852–4859, doi:10.1063/1.1674762, 1971. 6487, 6497
Nelson, D. D., Schiffman, A., Nesbitt, D. J., Orlando, J. J., and Burkholder, J. B.: $H+O_3$ Fourier-transform infrared-emisson and laser-absortion studies og OH($X^2\Pi$) radical: An experimental dipole-moment function and state-to-state Einstein A coefficients coefficients, Chem. Phys. Lett, 93, 7003–7019, doi:10.1063/1.459476, 1990. 6497
Ohoyama, H., Kasai, T., Yoshimura, Y., and Kuwata, H.: Initial distribution of vibration of the OH radicals produced in the $H+O_3 \rightarrow OH(X^2\Pi_{1/2,3/2})+O_2$ reaction - Chemiluminescence by a crossed beam technique, Chem. Phys. Lett., 118, 263–266, doi:10.1016/0009-2614(85)85312-4, 1985. 6487, 6499
Pastrana, M. R., Quintales, L. A. M., Brandão, J., and Varandas, A. J. C.: Recalibration of a single-valued double many-body expansion potential-energy surface for ground-state HO_2 and dynamics calculations for the O+OH → O2+H reaction, J. Phys. Chem., 94, 8073–8080, doi:10.1021/j100384a019, 1990. 6490
Pickett, H. M. and Peterson, D. B.: Comparison of measured stratospheric OH with prediction, J. Geophys. Res., 101, 16789–16796, doi:10.1029/96JD01168, 1996. 6488
Pickett, H. M., Read, W. G., Lee, K. K., and Young, Y. L.: Observation of night OH in the mesosphere, Geophys. Res. Lett., 33, L19808, doi:10.1029/2006GL026910, 2006. 6489
Sander, S. P., Orkin, V. L., Kurylo, M. J., Golden, D. M., Huie, R. E., Kolb, C. E., Finlayson-Pitts, B. J., Molina, M. J., Friedl, R. R., Ravishankara, A. R., Moortgat, G. K., Keller-Rudek, H., and Wine, P. H.: Chemical Kinetics and Photochemical Data for Use in Atmospheric Studies, Evaluation Number 15, Jet Propulsion Laboratory, Pasadena, CA, 2006. 6492
Silveira, D. M., Caridade, P. J. S. B., and Varandas, A. J. C.: Dynamics of the $O+HO_2$ reaction using two DMBE potential energy surfaces: The role of vibrational excitation, J. Phys. Chem. A, 108, 8721–8730, doi:10.1021/jp049575z, 2004. 6487, 6494
Slanger, T. G., Jusinski, L. E., Black, G., and Gadd, G. E.: A new laboratory source of ozone and its potential atmospheric implications, Science, 241, 945–950,

ACPD
12, 6485–6517, 2012

doi:10.1126/science.241.4868.945, 1988. 6486
Smith, I. W. M., Herbst, E., and Chang, Q.: Rapid neutral-neutral reactions at low temperatures: A new network and first results for TMC-1, Mon. Not. R. Astron. Soc., 350, 323–330 , doi:10.1111/j.1365-2966.2004.07656.x, 2004. 6489
Spencer, J. E. and Glass, G. P.: Some reactions of OH($v = 1$), Int. J. Chem. Kin., 9, 111–122 , doi:10.1002/kin.550090110, 1977. 6489, 6492
Spitzer Jr., L.: The terrestrial atmosphere above 300 km, in: The Atmospheres of the Earth and Planets, (Ed.), 213, Univ. Chicago Press, Chicago., USA, 1949. 6486
Steinfeld, J. I., Adler-Golden, S. M., and Gallagher, J. W.: Critical survey of data on the spectroscopy and kinetics of ozone in the mesosphere and thermosphere, J. Phys. Chem. Ref. Data, 16, 911–951, doi:10.1063/1.1674762, 1987. 6497
Toumi, R., Kerridge, B. J., and Pyle, J. A.: Highly vibrationally excited oxygen as a potential source of ozone in the upper-stratosphere and mesosphere, Nature, 351, 217–219, doi:10.1038/351217a0, 1991. 6486
Toumi, R., Houston, P. L., and Wodtke, A. M.: Reactive $O_2(v \geq 26)$ as a source of stratospheric ozone, J. Chem. Phys., 104, 775–776, doi:10.1063/1.471642, 1996. 6486
Turnbull, D. N. and Lowe, R. P.: New hydroxyl transition probabilities and their importance in airglow studies, Planet Space Sci., 37, 723–738 , doi:10.1016/0032-0633(89)90042-1, 1989. 6497
van der Loo, M. P. J. and Groenenboom, G.: Theoretical transition probabilities for the OH Meinel system, J. Chem. Phys., 126, 114314 , doi:10.1063/1.2646859, 2007. 6497, 6498
van der Loo, M. P. J. and Groenenboom, G.: Theoretical transition probabilities for the OH Meinel system, J. Chem. Phys., 126, 159902, doi:10.1063/1.2899016, 2008. 6497, 6498
Varandas, A. J. C.: Faraday Discuss. Chem. Soc., 84, 353–356 doi:10.1039/DC9878400351, 1987. 6492
Varandas, A. J. C.: On the ozone deficit problem: What are depletion cycles hiding?, Chem. Phys. Chem., 3, 433–441, doi:10.1002/1439-7641(20020517)3:5<433::AID-CPHC433>3.0.CO;2-O, 2002. 6486, 6494, 6500
Varandas, A. J. C.: Steady-state distributions of O_2 and OH in the high atmosphere, and implications in the ozone chemistry, J. Phys. Chem. A, 107, 3769–3777, doi:10.1021/jp022483u, 2003. 6486, 6490, 6499, 6500, 6512
Varandas, A. J. C.: Reactive and non-reactive vibrational quenching in O+OH collisions, Chem. Phys. Lett., 396, 182–190, doi:10.1016/j.cplett.2004.08.023, 2004a. 6489, 6490, 6491, 6492,

ACPD
12, 6485–6517, 2012

6493, 6495, 6502, 6515, 6516, 6517
Varandas, A. J. C.: Are vibrationally excited molecules a clue for the 'O_3 deficit problem' and 'HO_x dilemma' in the middle atmosphere?, J. Phys. Chem. A, 108, 758–769, doi:10.1021/jp036321p, 2004b. 6500, 6501, 6513
Varandas, A. J. C.: Reply to the comment on "Are vibrationally excited molecules a clue for the O-3 deficit problem and HOx dilemma in the middle atmosphere?", J. Phys. Chem. A, 109, 2700–2702, doi:10.1021/jp040745h, 2005a. 6500, 6501, 6503, 6513
Varandas, A. J. C.: What are the implications of non-equilibrium in the $O + OH$ and $O + HO_2$ reactions?, Chem. Phys. Chem., 6, 453–465, doi:10.1002/cphc.200400335, 2005b. 6486, 6487, 6490, 6494, 6495, 6500, 6503
Varandas, A. J. C.: Trajectory binning scheme and non-active treatment of zero-point energy leakage in quasi-classical dynamics, Chem. Phys. Lett., 439, 386–392, doi:10.1016/j.cplett.2007.03.090, 2007. 6489, 6490, 6491, 6492
Varandas, A. J. C. and Zhang, L.: $OH(v) + O_3$: Does chemical reaction dominate over non-reactive quenching?, Chem. Phys. Lett., 340, 62–70 , doi:10.1016/S0009-2614(01)00364-5, 2001. 6494
von Clarmann, T., Hase, F., Funke, B., López-Puertas, M., Orphal, J., Sinnhuber, M., Stller, G. P., and Winkler, H.: Do vibrationally excited OH molecules affect middle and upper atmospheric chemistry?, Atmos. Chem. Phys., 10, 9953–9964, doi:10.5194/acp-10-9953-2010, 2010. 6487, 6489
Wallace, L.: The OH nightglow emission, J. Atmos. Sci., 19, 1–16, doi:10.1175/1520-0469(1962)019<0001:TONE>2.0.CO;2, 1962. 6498
Xie, D., Xu, C., Ho, T., Rabitz, H., Lendvay, G., Lin, S. Y., and Guo, H.: Global analytical potential energy surfaces for $HO_2(\tilde{X}^2A'')$ based on high-level ab initio calculations, J. Chem. Phys., 126, 074315, doi:10.1063/1.2446994, 2007. 6490
Zhang, L. and Varandas, A. J. C.: Dynamics of the $OH(v = 1,2,4) + O_3$ atmospheric reaction, Phys. Chem. Chem. Phys., 3, 1439–1445, doi:10.1039/b010149o, 2001. 6494
Zhao, M., Truhlar, D. G., Blais, N. C., Schwenke, D. W., and Kouri, D. J.: Are classical molecular dynamics calculations accurate for state-to-state probabilities in $H + D_2$ reaction?, J. Phys. Chem., 94, 6696–6706, doi:10.1021/j100380a033, 1990. 6491

ACPD
12, 6485–6517, 2012

Table 1. State-to-state, state-to-all, and state-specific rate constants (multiplied by 10^{12}) for the O + OH(v) reaction.

	$k^{v'\to v''}_{(R5)}$/cm^{-3}s^{-1}										$k^{v'}_{(R4)}$/cm^{-3}s^{-1}	$\eta_v(T)$
v'	$v''=0$	1	2	3	4	5	6	7	8	all		
$T = 110$ K												
1	35.5									35.5	41.1	1.16
2	14.9	15.5								30.4	40.4	1.33
3	14.5	10.1	10.1							34.7	40.4	1.16
4	7.2	12.5	8.4	9.1						37.2	45.6	1.23
5	7.4	6.2	7.8	5.8	6.2					33.4	41.5	1.24
6	6.3	6.3	8.1	10.3	3.6	5.4				29.7	39.8	1.34
7	3.5	4.7	4.2	6.4	5.5	3.1	4.7			32.1	51.9	1.62
8	3.2	2.3	2.7	3.0	1.6	3.9	4.1	5.4		26.2	54.5	2.08
9	1.0	1.3	2.5	2.1	3.1	2.3	3.4	3.6	3.4	22.7	62.7	2.76
$T = 160$ K												
1	28.4									28.4	31.5	1.11
2	19.2	13.2								32.4	30.0	0.926
3	13.6	9.4	6.3							29.3	37.4	1.28
4	9.4	8.7	6.2	5.6						29.9	44.3	1.48
5	5.8	5.3	8.6	5.5	3.3					28.5	37.7	1.32
6	5.8	5.6	4.8	4.6	3.7	4.4				28.9	40.0	1.38
7	3.6	3.2	5.5	3.3	4.3	2.5	5.1			27.5	44.2	1.61
8	2.5	2.6	2.9	2.5	2.3	2.5	3.9	5.6		24.8	48.0	1.94
9	1.5	1.9	1.7	3.5	2.3	2.4	3.1	2.0	4.0	22.4	54.2	2.42
$T = 210$ K												
1	20.2									20.2	34.2	1.69
2	12.0	13.3								25.3	31.9	1.26
3	10.2	7.3	11.3							28.8	30.5	1.06
4	9.8	7.9	7.1	5.5						30.3	36.8	1.21
5	2.1	5.3	8.4	4.9	4.3					25.0	32.2	1.29
6	2.6	4.9	5.7	3.9	4.5	2.6				24.2	39.3	1.62
7	3.2	3.2	2.9	4.1	4.2	3.2	3.9			24.7	38.7	1.57
8	4.1	2.9	2.1	1.9	2.1	2.7	2.9	2.7		21.4	45.2	2.11
9	1.8	1.8	1.4	2.2	2.1	1.3	1.9	2.3	2.6	17.4	50.7	2.91

ACPD
12, 6485–6517, 2012

Table 1. Continued.

	$k^{v'\to v''}_{(R5)}/\mathrm{cm^{-3}s^{-1}}$										$k^{v'}_{(R4)}/\mathrm{cm^{-3}s^{-1}}$	$\eta_v(T)$
v'	$v''=0$	1	2	3	4	5	6	7	8	all		
$T=255$ K												
1	21.0									21.0	24.8	1.18
2	12.4	11.4								23.8	27.3	1.15
3	8.5	10.5	7.4							26.4	32.7	1.24
4	7.5	7.0	6.7	5.8						27.0	32.2	1.19
5	5.7	5.4	6.3	5.8	4.7					27.9	32.1	1.15
6	4.6	4.0	4.4	5.4	3.5	4.2				26.1	33.1	1.27
7	3.6	3.4	3.0	3.7	3.2	3.2	4.1			24.2	37.2	1.54
8	2.4	2.3	2.4	2.2	2.2	2.6	2.9	3.9		20.9	42.8	2.05
9	1.5	1.3	1.5	1.8	1.9	1.8	2.2	2.4	3.1	17.5	45.4	2.59
$T=300$ K												
1	19.2									19.2	21.1	1.10
2	14.2	10.5								23.8	23.9	1.00
3	9.4	9.6	8.1							25.8	28.4	1.10
4	6.4	7.8	6.9	4.8						25.4	28.8	1.13
5	6.3	4.7	6.0	3.8	3.8					24.6	31.7	1.29
6	4.6	4.4	5.0	4.7	4.1	4.5				27.4	29.7	1.09
7	3.4	3.1	3.6	3.3	3.5	3.1	4.0			25.2	34.9	1.38
8	2.4	2.3	2.4	2.4	2.1	2.7	3.0	4.2		22.3	39.3	1.76
9	1.2	1.3	2.1	1.8	2.0	1.7	1.8	2.1	3.3	18.2	43.4	2.38

ACPD
12, 6485–6517, 2012

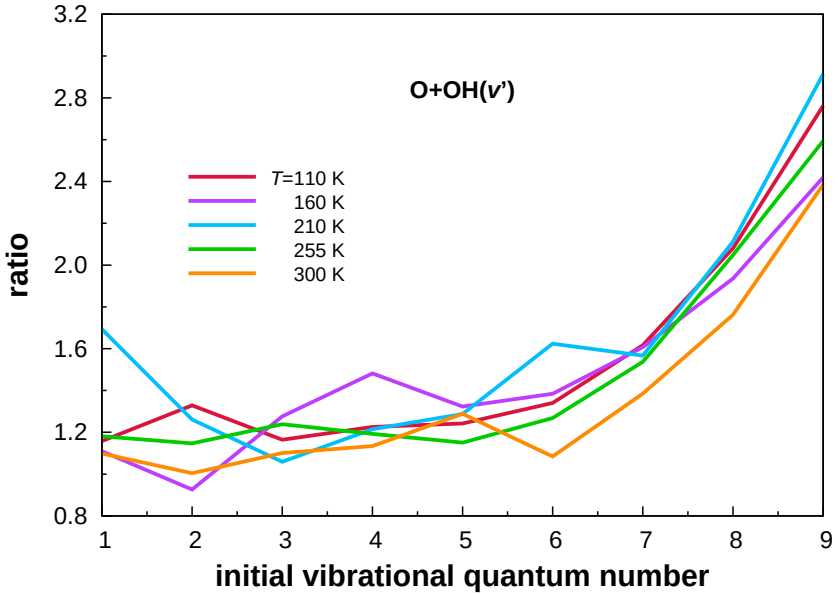

Fig. 1. Ratios between reactive and total vibrational relaxation as a function of the initial vibrational state of the hydroxyl molecule and temperature.

ACPD
12, 6485–6517, 2012

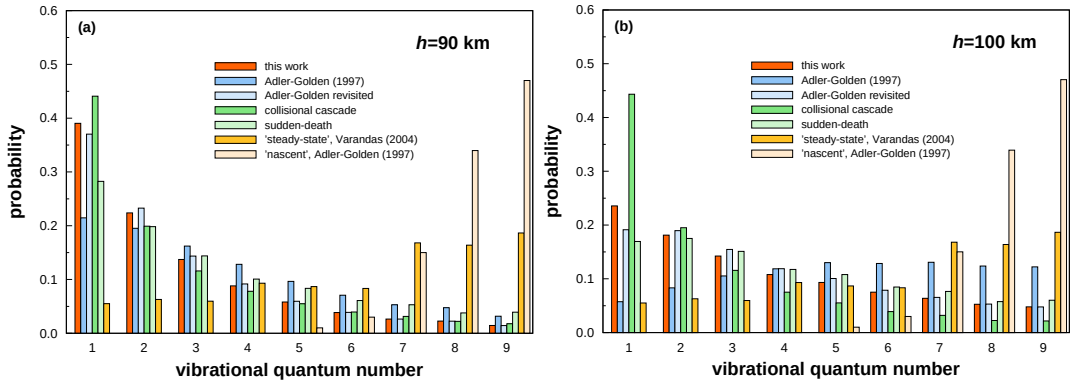

Fig. 2. Vibrational distributions of the hydroxyl radical at **(a)** 90 km and **(b)** 100 km. Also shown for comparison based on the same set of concentrations and rate-constants are: Adler-Golden (1997) results using his estimate for the O + OH(v) total rate constant; Adler-Golden scheme revisited using the effective rate constant based on this work; McDade and LLewellyn (1987) "sudden-death" and collisional cascade. Also included is other theoretical data of Varandas (2003) and the "experimental"-renormalized nascent distribution in Reaction (R8) of Charters et al. (1971).

ACPD
12, 6485–6517, 2012

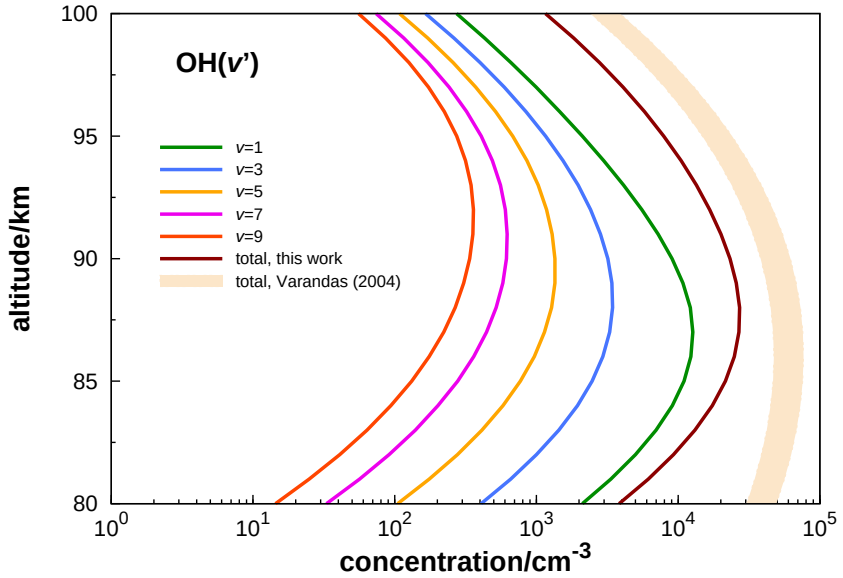

Fig. 3. Vertical profiles of vibrationally excited hydroxyl radical. The shaded area refers to the model reported elsewhere (Varandas, 2004b, 2005a) for the total concentration using satellite data taken in the equatorial region.

ACPD
12, 6485–6517, 2012

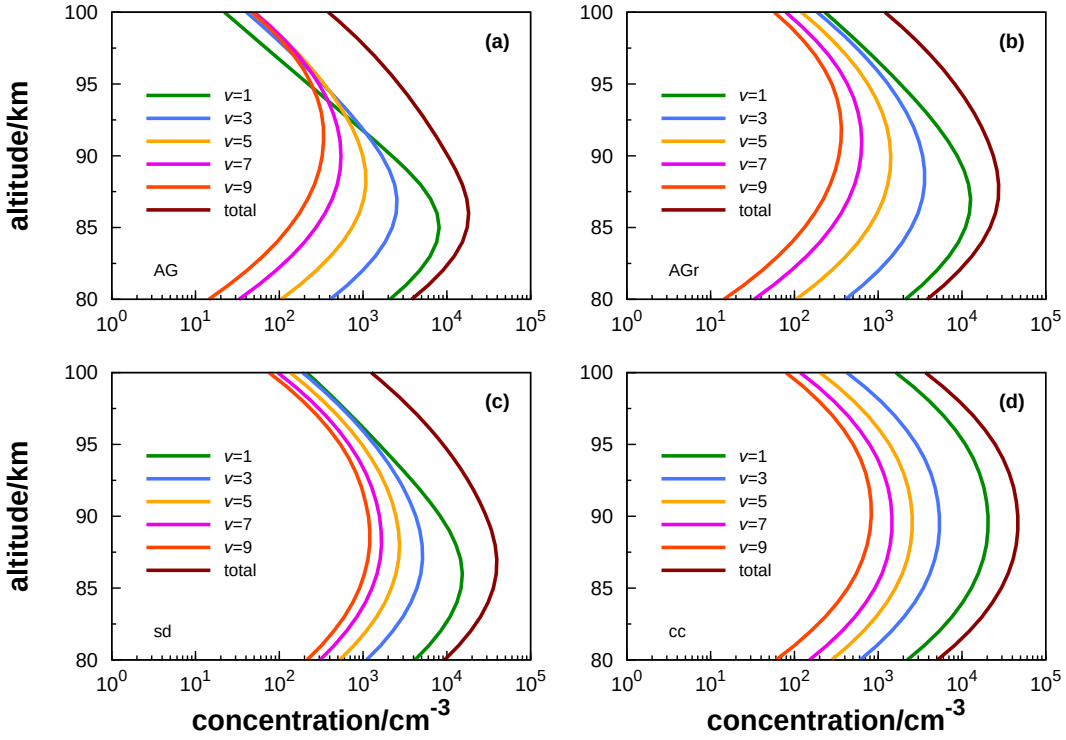

Fig. 4. Vertical profiles of vibrationally excited hydroxyl radical: **(a)** using the Adler-Golden (1997) O + OH(v) total rate constant; **(b)** Adler-Golden scheme revisited using the total rate constant from the current work; **(c)** McDade and LLewellyn (1987) "sudden-death" and **(d)** collisional cascade mechanisms.

ACPD
12, 6485–6517, 2012

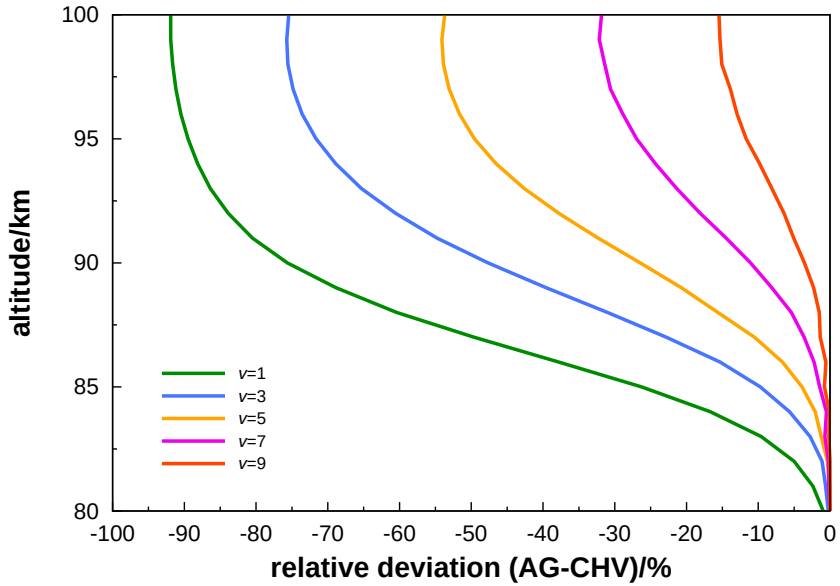

Fig. 5. Vertical profiles of differences between the results obtained with the empirical $O + OH(v')$ rate constant of Adler-Golden (1997) and the ones from the present work based on QCT calculations (Varandas, 2004a).

ACPD
12, 6485–6517, 2012

Implications of the O + OH reaction in hydroxyl nightglow modeling

P. J. S. B. Caridade et al.

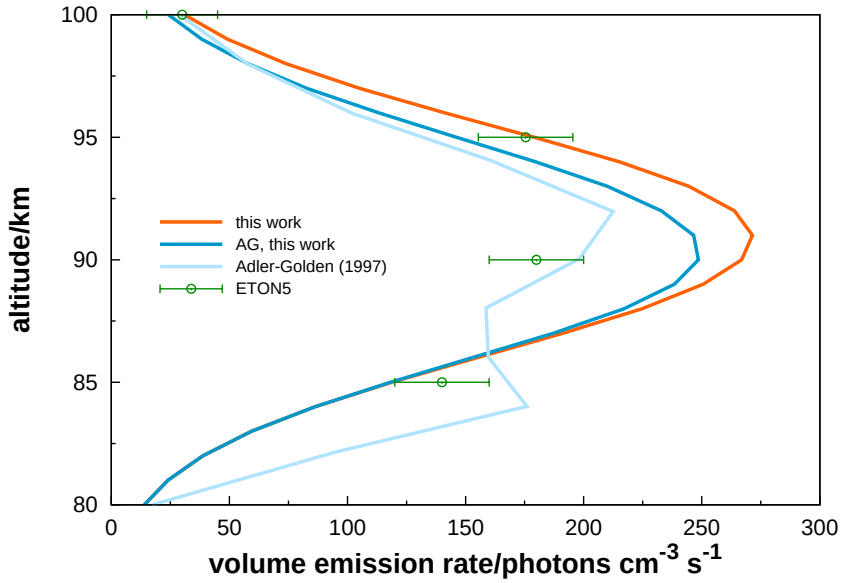

Fig. 6. Vertical profiles of the volume emission rate for the 8-3 band obtained using the empirical O + OH(v') rate constant from Adler-Golden (1997) and those from the present work based on the QCT calculations from Varandas (2004a). Also shown are the original reported data of Adler-Golden (1997) and the ETON5 experimental measurements (McDade et al., 1987).

ACPD
12, 6485–6517, 2012

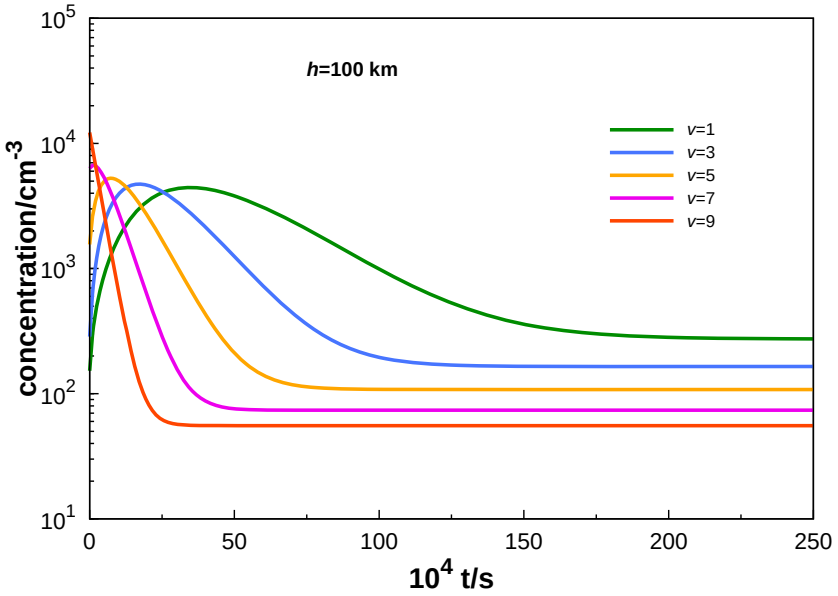

Fig. 7. Variation with time of the concentration of the various OH(v) species as integrated numerically using the QCT results from Varandas (2004a).

ACPD
12, 6485–6517, 2012

Implications of the O + OH reaction in hydroxyl nightglow modeling

P. J. S. B. Caridade et al.